World Conference on Timber Engineering Oslo 2023

SERVICEABILITY PERFORMANCE OF TIMBER DUAL FRAME-WALL STRUCTURAL SYSTEM UNDER WIND LOADING

Osama Abdelfattah Hegeir[1], Haris Stamatopoulos[2], Kjell Arne Malo[3]

ABSTRACT: Due to the moderate stiffness and low mass of timber multi-storey buildings, wind-induced accelerations and displacements usually govern the design. Moment-resisting timber frames (MRTFs) are structural systems that can provide open space and architectural flexibility. However, in regions with moderate to high wind velocities, MRTFs can be used for up to 8 storeys with small out-of-plane spacing between frames (C/C distance of the order of 2-3 m). In this paper, a dual frame-wall structural system is investigated. A parametric study using 2D linear elastic Finite Element Analysis (FEA) is performed to explore the feasibility of the system in regions with moderate wind velocities, considering serviceability requirements (lateral displacements and wind-induced accelerations). Floor vibrations are also taken into account. A 3D FEA model is used to verify the results of the 2D FEA model. Although the focus of the paper is devoted to serviceability requirements, some ultimate limit state considerations are discussed. The results highlight the possibility of using the dual system for multi-storey buildings, with up to 12 storeys and 5 m C/C distance in regions with basic wind velocities up to 26 m/sec.

KEYWORDS: Moment-resisting frames, serviceability, deflections, CLT, glulam, wind-induced accelerations, human-induced vibrations

1 INTRODUCTION

Timber has a very good strength/weight ratio due to its light weight compared to other building materials such as concrete and steel. Moreover, timber can be considered a more environment-friendly construction material than concrete and steel in terms of greenhouse gas emissions [1, 2]. Due to the lightweight nature and moderate stiffness of wood, timber structures are prone to serviceability problems such as excessive accelerations and displacements [3, 4]. Excessive accelerations can cause discomfort to the occupants, and excessive displacements can cause damage and therefore should be kept within acceptable limits.

There exist several structural systems that can provide lateral stiffness to a building. A common structural system used for tall timber buildings is diagonal bracing, such as Treet [4] and Mjøstårnet [5] in Norway. However, these buildings require huge bracing elements running along the height of the structure, which may compromise the architecture flexibility. Cross laminated timber (abbr. CLT) can also be used as a Lateral Load Resisting System (abbr. LLRS). An example of timber building with CLT walls is Stadthaus in London [6]. However, such structures are material-intensive, cellular, and can impose space limitations.

Open and flexible architectural design of buildings is a desirable property, which can be achieved by use of Moment-Resisting Timber Frames (abbr. MRTFs) as a LLRS. In MRTFs, the lateral stiffness relies largely on the stiffness of beam-to-column connections. A feasibility study of glulam MRTFs has been carried out by Vilguts et al. [3], showing that in high-wind regions, glulam MRTFs can hardly be used for more than 8 storeys. The study [3] assumes a prefabricated floor with a small 2.40 m out-of-plane spacing between adjacent frames (abbr. C/C). These limitations are due to wind-induced accelerations and lateral displacements [3].

To overcome the limitations on the number of storeys and achieve larger C/C distance, it is necessary to use larger columns and beams compared to standard glulam dimensions. CLT panels are currently produced with standard dimensions up to 3.5x16.0 m, and therefore can be used to achieve these larger dimensions.

In this paper, the feasibility of using dual frame-wall structural system to build up 12 storeys with C/C distance of 5 m considering a basic wind velocity of 26 m/sec is explored. The system consists of CLT walls, glulam columns and beams, and semi-rigid connections between beams and columns/walls. The feasibility of the system is evaluated, mainly, in terms of Serviceability Limit State (abbr. SLS). However, some Ultimate Limit State (abbr. ULS) considerations are also presented.

2 STRUCTURAL SYSTEM

In this section, the dual frame-wall structural system is explained. Both the LLRS and floor system are described in two different subsections.

[1] Osama Abdelfattah Hegeir osama.a.s.a.hegeir@ntnu.no
[2] Haris Stamatopoulos haris.stamatopoulos@ntnu.no
[3] Kjell Arne Malo kjell.malo@ntnu.no
Department of Structural Engineering, Norwegian University of Science and Technology (NTNU)

https://doi.org/10.52202/069179-0384

2.1 LATERAL LOAD RESISTING SYSTEM

An example of the structural system is shown in Figure 1 (a). In this paper, the focus is given to the structural system in X direction (marked with dotted red box in Figure 1 (a)) where the dual system is used. It consists of continuous CLT walls, continuous glulam columns, and glulam beams. Semi-rigid connections using threaded rods are assumed between beams and walls/columns (see Figure 1 (b)). More details on the connections using threaded rods can be found in [7]. In Y direction, the building may be stabilized by use of diagonal bracing. The LLRS is discussed in more detail in section 4.

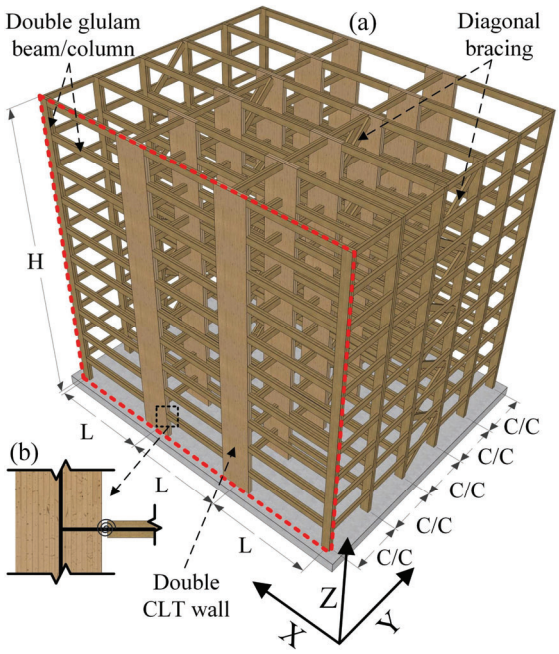

Figure 1: *(a) 3D view of the structural system, (b) semi-rigid moment connection*

2.2 FLOOR SYSTEM

In this paper, a ribbed slab floor system is assumed, see Figure 2. The system consists of CLT panels resting on simply supported secondary beams (glulam). The secondary beams are supported on the main LLRS working in X direction. The floor system is one way with load bearing parallel to Y axis. For better acoustic performance, double beams, columns, and walls are considered. Analysis of floors is discussed in section 3.

3 ANALYSIS OF FLOORS

Human-induced vibrations can be decisive in the design of timber floors [8, 9]. This section explores the serviceability performance of the floor system shown in Figure 2, which includes satisfying deflection limits and human-induced vibrations. However, the vibrations were found to be more critical than deflections. Therefore, the performance was only evaluated with respect to human-induced vibrations.

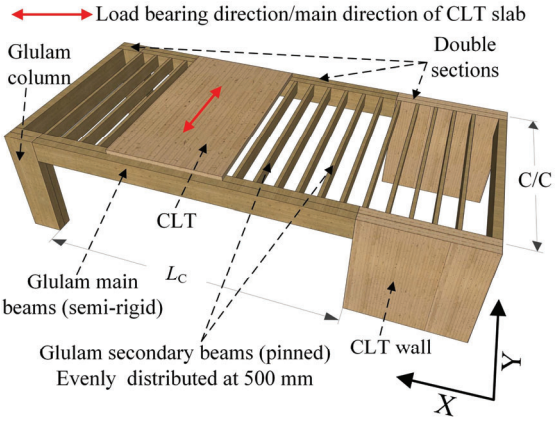

Figure 2: *Floor system*

Linear elastic Finite Element Analysis (abbr. FEA) was used to calculate the fundamental frequency and the deflection of the floor under unit load. The clear span L_C (confer Figure 2) and the stiffness of main beams' connections (confer Figure 2) were varied. The vibration performance of the floor was evaluated using the simplified Hu and Chui criterion [8].

3.1 MATERIALS

The glulam beams used in the floor is assumed of strength class GL30c as defined by EN 14080 [10]. The boards constituting the CLT panels are assumed of strength class C24 as defined by EN 338 [11]. In this paper, it was assumed that (2/3) of the boards are parallel to the main direction of CLT panels (confer Figure 2). The remaining (1/3) are orthogonal to the main direction. Table 1 summarizes mean stiffness properties for GL30c and C24, and the corresponding material axes are illustrated in Figure 3.

Table 1: *Mean stiffness properties for floor elements*

	GL30c	C24	Unit
E_1	13000	11000	N/mm^2
E_2	300	370	N/mm^2
E_3	300	370	N/mm^2
G_{12}	650	690	N/mm^2
G_{13}	650	690	N/mm^2
G_{23}	65	69	N/mm^2

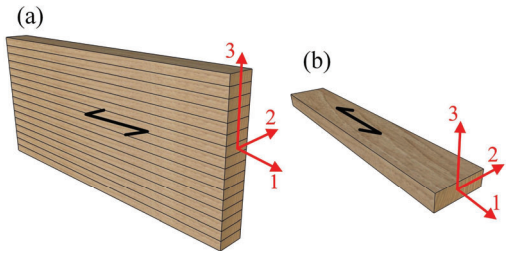

Figure 3: *Material axes for (a) glulam GL30c, (b) C24 boards*

https://doi.org/10.52202/069179-0384

3.2 FINITE ELEMENT MODELLING

CSI SAP2000 [12] was used for FEA. The software can be automated using Open Application Programming Interface (abbr. OAPI). The FEA model of the floor is shown in Figure 4. The main beams (glulam) are modelled using linear beam elements. The ends of the main beams are partially released with respect to bending moment to consider the semi-rigid connections. The secondary beams (glulam) are modelled using shell elements (shown in blue in Figure 4). The CLT slabs are modelled using layered shell elements (shown in red in Figure 4). The connections between the CLT slab and secondary beams, and the connections between the secondary beams and the main beams are modelled using link elements with only axial and shear stiffness (no rotational stiffness).

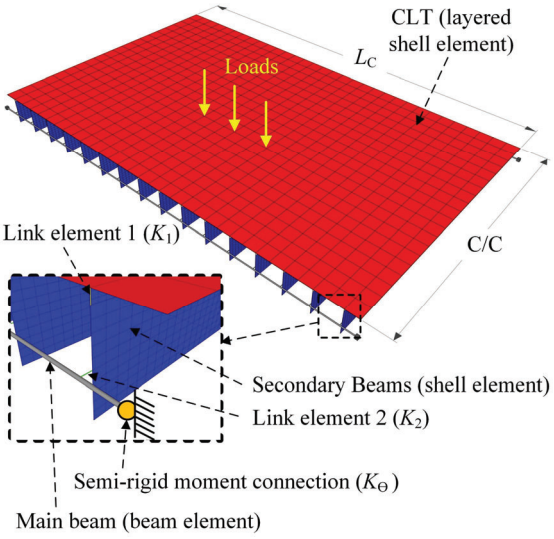

Figure 4: *FEA model of the floor*

3.3 ACCEPTANCE CRITERIA

Several design criteria exist for assessing floor vibrations caused by human activity (e.g. [8, 13]), each taking into account different factors and making different assumptions. In this paper, the simplified criterion proposed by Hu and Chui [8] is used:

$$\frac{(f_{n,1}/18.7)^{2.27}}{w_{1\,kN}} \geq 1.0 \qquad (1)$$

Where $f_{n,1}$ and $w_{1\,kN}$ are the fundamental frequency and the static deflection due to 1.0 kN.

The criterion [8] was developed based on testing of more than one hundred timber floors. Although this criterion [8] was developed in Canada, it is based on physical and subjective evaluations of floors with damping properties comparable to wooden floors found in Norway [14].

3.4 PARAMETRIC STUDY

A parametric study was performed to evaluate the performance of the floor. The parameters varied are summarized in Table 2. Two load scenarios are investigated, namely: heavy load, and light load, see Table 3. The heavy floors represent a case where additional mass is added to improve the performance of the building with respect to wind-induced accelerations (discussed in section 4).

The fundamental frequency $f_{n,1}$ used in evaluating human-induced vibration (see equation (1)) is calculated assuming only the dead load is applied to the CLT slab.

The connections between the CLT slab and the secondary beams, as well as the connections between the secondary beams and the main beams are assumed of equal translational stiffness K_1 and K_2 respectively, confer Figure 4 and Table 2. The main beams connection stiffness K_Θ is reasonably assumed based on the experimental work performed by Vilguts et al. [7] and the analytical work done by Stamatopoulos et al. [15]. Two sets of beams cross-sections and CLT layups are used depending on the load scenario, see Table 4. In total, 60 3D linear elastic analyses were performed.

Table 2: *Parameters used in the parametric study of the floors*

	Value(s)	Unit
Clear span L_C	7−9	m
C/C	5	m
K_Θ	0−15,000	kN·m/rad
K_1*	10	kN/mm
K_2	20	kN/mm
Damping ratio (ξ)	2	%

* Evenly distributed at 250 mm

Table 3: *Load scenarios*

	Heavy load	Light load	Unit
Dead load G_k*	2.0	1.0	kN/m^2
Live load Q_k	3.0**	2.0***	kN/m^2

* Including the own weight of beams and slabs
** Office buildings as defined by EN 1991-1-1 [16]
*** Residential buildings as defined by EN 1991-1-1 [16]

Table 4: *Beams cross-sections and CLT layups used in the parametric study of the floors*

	Load scenario	Cross-section/layup	Unit
Main beam	Heavy/light	$215 \cdot 585$	mm^2
Sec. beam	Heavy	$115 \cdot 450$	mm^2
CLT slab		30/30/30	mm
Sec. beam	Light	$90 \cdot 450$	mm^2
CLT slab		40/40/40	mm

Figure 5 shows the performance of the floor according to Hu and Chui [8] as function of the clear span L_C. As shown in Figure 5, for $K_\Theta = 15{,}000$ kN·m/rad, light floors with clear span up to 8.5 m and heavy floors with clear span up to 7.5 meet the acceptance limit. For $K_\Theta = 0$ (pinned), only light floors with clear span of 7.0 m meet the limit.

According to EN 1995-1-1 [17], special investigation is needed for residential timber floors with fundamental frequency less than 8 Hz. Modal analysis is used to calculate the fundamental frequency assuming only dead

load is applied to the CLT slab. The frequencies of light and heavy floors are shown in Figure 6. For floors with $K_\theta = 15{,}000$, the frequencies of all light floors meet the acceptance limit (8 Hz), while only heavy floors with clear span ≤ 7.5 m meet the limit. For floors with $K_\theta = 0$, only light floors with clear span ≤ 8.5 m meet the frequency limit.

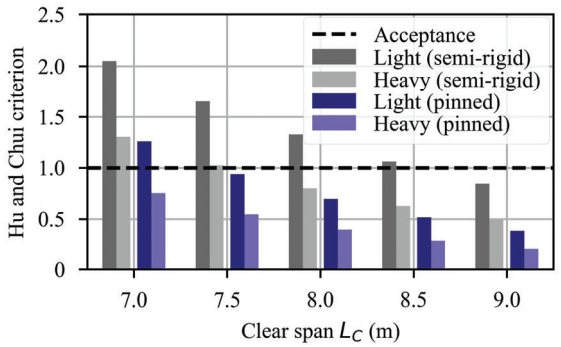

Figure 5: *Hu and Chui [8] criterion for human-induced vibrations (pinned: K_θ=0, and semi-rigid: K_θ=15,000 kN·m/rad)*

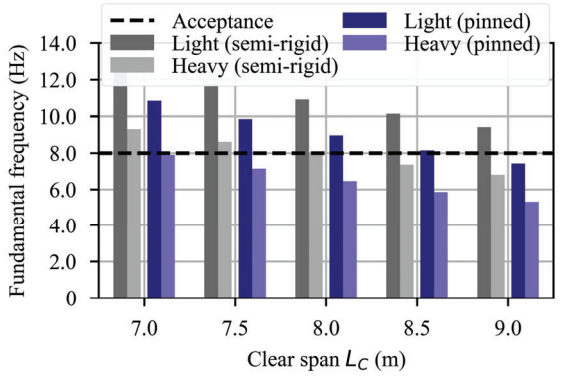

Figure 6: *Fundamental frequencies of floors (pinned: K_θ=0, semi rigid: K_θ=15,000 kN·m/rad, and only the dead load is considered)*

According to Hu and Chui criterion [8], and in compliance with EN 1995-1-1 [17] requirement of a minimum frequency of 8 Hz, some conclusions can be drawn from the parametric study (see Table 2):

- Light floors with clear span ≤ 8.5 m satisfy the requirements given that $K_\theta \geq 15{,}000$ kN·m/rad.
- Heavy floors with clear span ≤ 7.5 m satisfy the requirements given that $K_\theta \geq 15{,}000$ kN·m/rad.
- If pinned connections are used ($K_\theta = 0$), only light floors with clear span ≤ 7 m meet the requirements.

The influence of main beam connection stiffness (K_θ) on frequency and vibration performance is shown in Figure 7, where the rotational stiffness (K_θ) is varied from 0 (pinned) to 15,000 kN·m/rad for a light floor with a clear span of 8 m. As depicted in Figure 7, an increase in K_θ results in a higher floor frequency and improved vibration performance, owing to the increased floor stiffness.

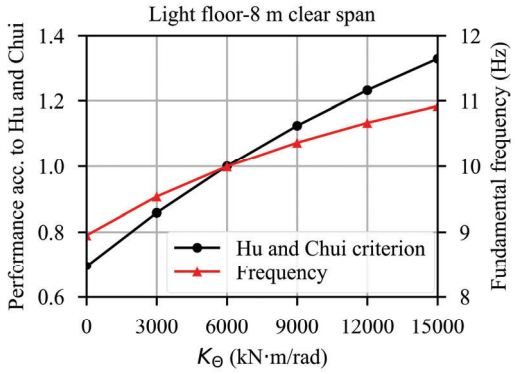

Figure 7: *Influence of main beams connections' stiffness on frequency and vibration performance as per Hu and Chui [8]*

4 ANALYSIS OF LATERAL LOAD RESISTING SYSTEM

Figure 1 shows a 3D structural system with X and Y directions perpendicular to each other. In this section, a small parametric study is performed to evaluate the feasibility of the dual frame-wall LLRS (in X direction) using 2D linear elastic FEA. Although the feasibility is evaluated primarily with respect to SLS, some ULS considerations are discussed. To validate the conclusions drawn from the 2D FEA, a 3D linear elastic FEA model was prepared, and the results were compared with those of the 2D FEA model.

Intuitively, higher connections' stiffness is required at lower storeys. The possibility of using lower connections' stiffness at the higher storeys is also explored.

4.1 MATERIALS

The LLRS in X direction consists of glulam beams, glulam columns, and CLT walls. The stiffness properties of glulam are the same as the floor (see Table 1).

A simplified modelling approach of CLT is to model CLT using equivalent stiffness properties assuming homogeneous cross-section with grain direction of all layers parallel to stress direction as proposed by [18]. This simplified modelling of CLT has shown good accuracy for CLT loaded in-plane [19]. Similar to the floors, 2/3 of the boards are assumed parallel to the main direction of CLT panels and the remaining 1/3 are orthogonal to the main direction. Equivalent stiffness properties of CLT walls are summarized in Table 5. The corresponding material axes are shown in Figure 8. Since linear elements were used to model the CLT walls (explained in 4.2 in this paper), only E_1 and G_{12} are relevant (confer Figure 8). E_1 affects the vertical axial stiffness and the bending stiffness of the CLT walls, and G_{12} affects their in-plane shear stiffness.

Table 5: *Equivalent stiffness properties of CLT walls*

	Equivalent stiffness	Unit
E_1	7457	N/mm²
G_{12}	518	N/mm²

https://doi.org/10.52202/069179-0384

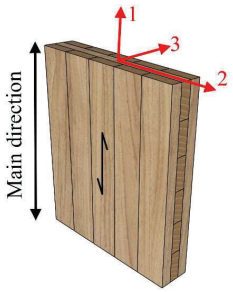

Figure 8: *Material axes for CLT walls*

4.2 FINITE ELEMENT MODELLING

Figure 9 shows the FEA model of the dual frame-wall system (X direction). CSI SAP2000 [12] was used to perform 2D linear elastic FEA. Glulam columns and beams were modelled using linear beam elements with the stiffness properties in Table 1. The CLT walls were also modelled using linear beam elements with the equivalent properties in Table 5. The linear beam elements representing the CLT walls were verified against the layered shell elements available in CSI SAP2000 [12] under in-plane loading. The verification was done on both stresses and displacements and the difference was less than 5%. Hence, linear beam elements were deemed to have sufficient accuracy for the purpose of this study.

All connections (beam-column/wall, wall-foundation, and column-foundation) were modelled using moment partial release available in CSI SAP2000 [12], and were considered semi-rigid with respect to moment and rigid with respect to translation.

Columns and walls have finite heights (in-plane dimension of the cross-section), therefore, when modelled using linear elements, beams' spans are increased. To account for this increase, end-length offset available in CSI SAP2000 [12] is used, see Figure 9. At each end of the beam, a length equal to half the column/wall height is assumed rigid for bending and shear deformations.

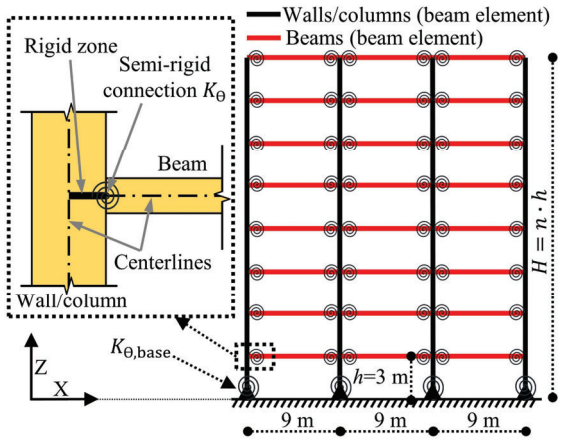

Figure 9: *2D FEA model of LLRS in X direction*

4.3 PARAMETRIC STUDY

In this parametric study, two variations of the LLRS in X direction shown in Figure 9 are considered, namely: exterior CLT walls, and interior CLT walls, see Figure 10. Both heavy and light loading scenarios are considered (see Table 3). The dead load in Table 3 includes the weight of the floor, while the own weight of LLRS is automatically calculated by CSI SAP2000 [12]. The parameters of the parametric study are summarized in Table 6 (total of 520 analyses).

The cross-sections of walls and columns, and the stiffness of their connections to the foundation were varied according to the number of storeys n, see Table 7. All beams, columns, and walls are double sections, confer Figure 2. The cross-sections and stiffness values in Table 6 and Table 7 are for single cross-section.

Table 6: *Parameters of the parametric study of the LLRS*

Parameter	Value(s)
Number of storeys (n)	4/6/8/10/12
Number of bays (n_b)	3
Gravity loads	Light/heavy
Variation	Interior/exterior CLT
C/C (Figure 1)	5 m
Basic wind velocity	26 m/sec
Beams	$215 \cdot 585$ mm^2
Beam-column/wall connection stiffness (K_Θ)	2,500-15,000 kN·m/rad

Table 7: *Cross-section of columns and walls and the stiffness of their connection to foundation (n: number of storeys)*

	n	Cross-sec. (mm^2)	$K_{\Theta,base}$ (kN·m/rad)
Glulam columns	12	$215 \cdot 720$	5,000
	10	$215 \cdot 630$	3,750
	8	$215 \cdot 540$	2,500
	6	$215 \cdot 450$	1,250
	4	$215 \cdot 450$	1,250
CLT walls	12	$215 \cdot 3500$	200,000
	10	$215 \cdot 3000$	150,000
	8	$215 \cdot 2500$	100,000
	6	$215 \cdot 2000$	60,000
	4	$215 \cdot 1500$	30,000

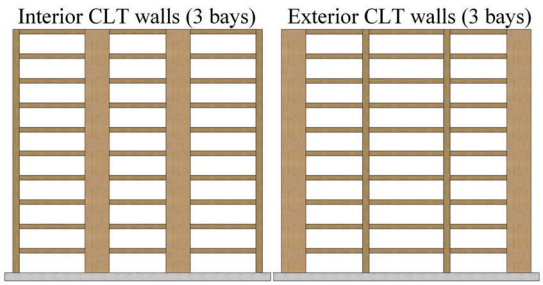

Figure 10: *Two variations of LLRS in X direction*

4.3.1 Serviceability performance

The serviceability performance of LLRS is evaluated in terms of wind-induced accelerations, top floor displacement (abbr. Disp.), and inter-storey drift (abbr. IDR). For the calculation of lateral displacements (Disp. and IDR) due to wind loading (W_k), the characteristic load

combination as defined in EN 1990 [20] with wind as a leading variable was used:

$$E_{\mathrm{d}} = G_{\mathrm{k}} + W_{\mathrm{k}} + \psi_0 \cdot Q_{\mathrm{k}} \quad (2)$$

The combination factor ψ_0 was set to 0.70 according to EN 1990 [20].

Some recommendations of deflections limits are provided by EN 1995-1-1 [17]. According to these recommendations, deflections in simple beams under characteristic load combination defined in EN 1990 [20] should be limited to $1/300 - 1/500$ of the span. No recommendations are given on structure level. As an approximation, the limits for simple beams are used for both lateral displacement at the top of the building (Δ) and relative displacement between two successive storeys (δ):

$$\Delta \leq {}^{H}/_{300}, \delta \leq {}^{h}/_{300} \quad (3)$$

Where h is the height of a storey and H is the total height of the building.

For the calculations of wind-induced accelerations, procedure 1 in Annex B of EN 1991-1-4 [21] was used. The procedure is based on gust factor approach. For the calculation of wind-induced accelerations according to EN 1991-1-4 [21], the mode shape, and the fundamental frequency are required. To obtain both the mode shape and the fundamental frequency, modal analysis using CSI SAP2000 [12] was performed. In the modal analysis, the mass is calculated using the quasi-permanent load combination defined in EN 1990 [20]:

$$E_d = G_k + 0.3 \cdot Q_k \quad (4)$$

Damping is an important input to the wind-induced acceleration calculation. Little research has been done on damping of timber structures, see e.g. [22]. In this paper, 2% damping ratio (ξ) was assumed based on [22]. Basic wind velocity of 26 m/sec and urban environment (IV) as defined by EN 1991-1-4 [21] were assumed for the calculation of wind loads and wind-induced accelerations. Relevant parameters used in the calculation of wind-induced accelerations are summarized in Table 8.

Table 8: *Relevant parameters for calculation of wind loads and wind-induced accelerations*

Parameter	Value
Directional factor C_{dir}	1.0
Seasonal factor C_{season}	1.00
Probability factor C_{prob}	0.73
Orography factor $C_{0(\mathrm{z})}$	1.00
Turbulence factor k_{l}	1.00
Terrain category	IV
Reference height Z_{t}	200
Reference length L_t	300
Structural damping ξ	2%
Width of the building ($C/C \cdot 5$)	25 m

In this paper, the wind-induced acceleration acceptance criterion of ISO 10137 [13] is used. The criterion covers the range from a fundamental frequency of 0.063 to 5 Hz for a maximum wind velocity with a return period of one year, for both residential and office buildings.

Figure 11 shows the wind-induced accelerations against ISO 10137 criterion [13] for all frames (see Table 6). Figure 12 shows the maximum and minimum lateral displacements and IDR for all frames (see Table 6), where maximum and minimum correspond to a set of frames with common parameters and K_θ =2,500 kN·m/rad and 15,000 kN·m/rad respectively. Light and heavy frames have the same lateral displacements since gravity loads have no influence on lateral displacements.

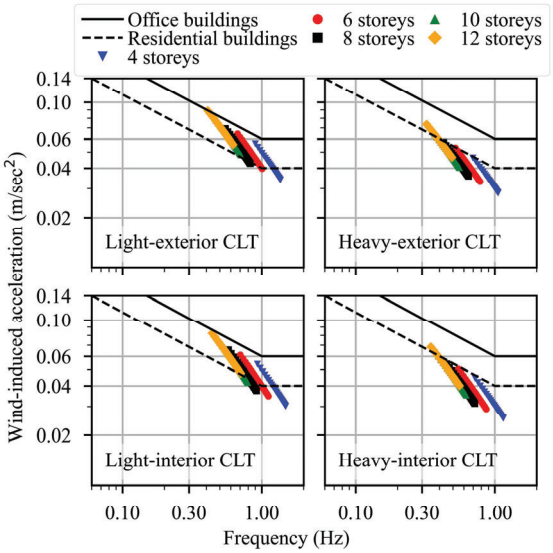

Figure 11: *Wind-induced accelerations against ISO 10137 [13] criterion*

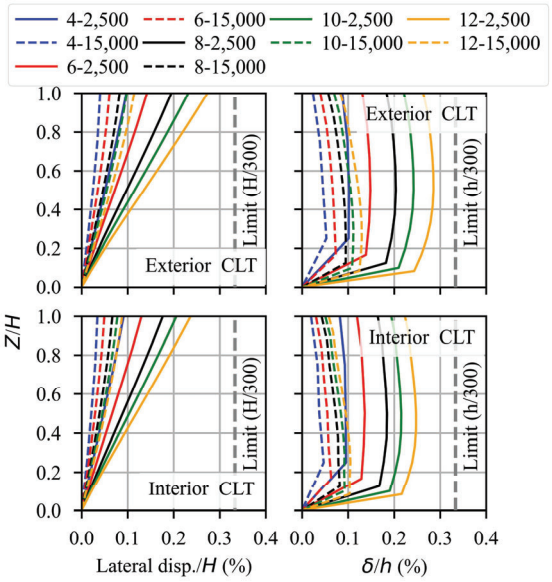

Figure 12: *Lateral displacements and inter-storey drift (Legend: number of storeys-K_θ, and Z: height above ground)*

As shown in Figure 11 and 12, the variation with interior CLT walls is slightly outperforming the variation with exterior CLT walls. The variation with interior CLT walls has 5-10% lower wind-induced accelerations and 5-15%

https://doi.org/10.52202/069179-0384

lower lateral displacements. Frames with heavy loads have 20% lower wind-induced accelerations.
Observing Figure 11 and Figure 12, some conclusions can be made:

- All frames satisfy the requirements of top floor displacement and IDR by a good margin.
- Heavy frames up to 12 storeys meet the requirement of residential buildings provided that $K_\theta \geq 2 \cdot 5{,}500$ kN·m/rad (5,500 for single cross-section).
- Light frames up to 10 storeys meet the requirement of residential buildings provided that $K_\theta \geq 2 \cdot 11{,}500$ kN·m/rad (11,500 for single cross-section).
- Light frames of 12 storeys do not meet the requirement of residential buildings.
- Light and heavy frames up to 12 storeys meet the requirement of office buildings provided that $K_\theta \geq 2 \cdot 2{,}500$ kN·m/rad (2,500 for single cross-section).

4.3.2 Stiffness reduction in higher storeys

Connections with high stiffness are intuitively required at lower storeys, and connections with lower stiffness may be used in upper storeys. To verify such hypothesis, a 10-storey frame, with interior CLT walls and light gravity loads, is selected as a benchmark. All other parameters remain the same (see Tables 5-7).
A rotational stiffness (K_θ) of 5,000 kN·m/rad is assigned to all beam-to-column/wall connections, this is referred to as the reference case. High stiffness of (K_θ) 15,000 kN·m/rad is then assigned to all connections of one floor at each step starting from the bottom up (total of 10 steps). At the final step, all connections have a stiffness (K_θ) of 15,000 kN·m/rad. The case of all connections being rotationally rigid is also shown. In total, 12 analyses were performed. Figure 13 shows the top floor displacement, maximum IDR, and wind-induced acceleration, all normalized to the reference case ($K_\theta = 5{,}000$ kN·m/rad). In Figure 13, a value of 0 at the horizontal axis represents all connections with stiffness of 5,000 kN·m/rad (reference case), while a value of 10 represents all connections with a stiffness of 15,000 kN·m/rad.

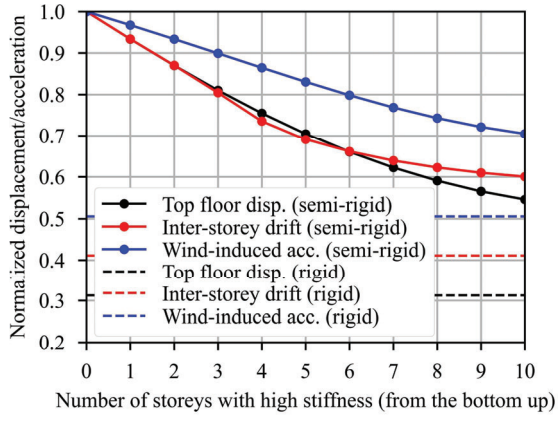

Figure 13: *Top floor displacement, maximum IDR, and wind-induced acceleration with variable K_θ (higher at lower storeys) normalized to the reference case ($K_\theta = 5{,}000$ kN·m/rad).*

As shown in Figure 13, IDR shows the fastest convergence, followed by top floor displacement and wind-induced acceleration. Using high stiffness (K_θ =15,000 kN·m/rad) for the bottom 5-6 storeys results in 70-90% of the reduction in lateral displacements (top floor displacement and IDR) compared to the case with all connections of high stiffness (10 at the horizontal axis of Figure 13). Using high stiffness for the bottom 5-6 storeys results in 60-70% of the reduction in wind-induced acceleration compared to the case with all connections of high stiffness.

4.3.3 Ultimate limit state considerations

The results of the parametric study (520 analyses) are used to perform design checks for beams, columns, and CLT walls. For the calculation of forces used in the design, the fundamental ULS combination defined in EN 1990 [20] with wind as leading variable action was used:

$$E_\mathrm{d} = \gamma_\mathrm{G} \cdot G_\mathrm{k} + \gamma_\mathrm{Q} \cdot W_\mathrm{k} + \gamma_\mathrm{Q} \cdot \psi_0 \cdot Q_\mathrm{k} \qquad (5)$$

Where $\gamma_\mathrm{G} = 1.20$, $\gamma_\mathrm{Q} = 1.50$, $\psi_0 = 0.70$.
The structural design was performed in accordance with EN 1995-1-1 [17]. Since no CLT design checks are included in EN 1995-1-1 [17], the design checks of CLT walls were performed according to [23]. The buckling length was evaluated using linearized buckling analysis. The utilization ratios for beams, columns, and CLT walls are shown in Figure 14 for a total of 520 analyses. As shown in Figure 14, all utilization ratios of beams, columns, and walls are well below unity.

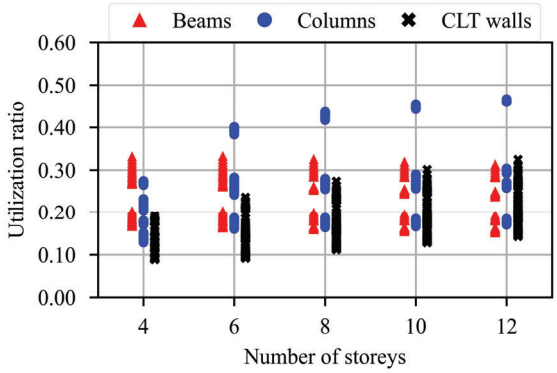

Figure 14: *Utilization ratio for beams, columns, and CLT walls*

Another important consideration is the beam-column/wall connection capacity. For each analysis case (out of the 520), bending moments are calculated at all connections in the frame, the maximum absolute value is then selected, the results are shown in Figure 15.
As shown in Figure 15, all moments are below 70 kN·m. An experimental work performed on moment resisting connections based on threaded rods [24] reported capacity up to 130 kN·m with glulam beams and columns of dimensions ($140 \cdot 450$ mm^2). Based on the calculated bending moments (see Figure 15), and the results in [24], the connections in the dual frame-wall system seem feasible. However, the reported testes in [24] were performed on glulam beam-column connections. Moreover, the limited number of experiments performed

on such connections does not allow the estimation of characteristic capacity. Therefore, further experimental work on moment resisting connections using threaded rods and CLT is needed.

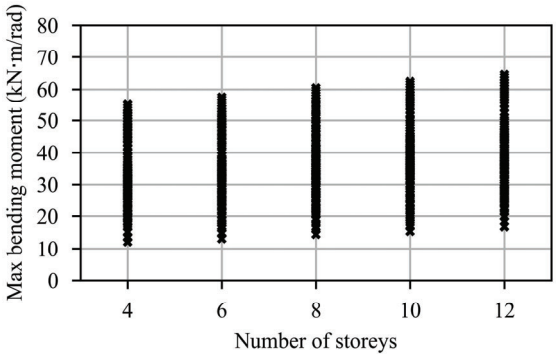

Figure 15: *Maximum absolute bending moment at all beam-to-column/wall connections*

4.4 3D STRUCTURE

To verify the results of the 2D FEA analysis performed in the parametric study, the dual frame-wall system is analysed in 3D. A 3D FEA model of an 8-storey building is analysed using CSI SAP2000 [12].

In X direction, the building is stabilized using the dual frame-wall system with interior CLT walls (confer Figure 1 and Figure 9). The beam-to-column/wall connection stiffness (K_θ) is set to $2 \cdot 12{,}500$ kN·m/rad (double cross-section), see Figure 9.

In Y direction, the building is stabilized using diagonal bracing (confer Figure 1 and Figure 16). The diagonals are modelled using link elements with axial stiffness only. The axial stiffness of each link element representing a diagonal is assumed to be 100 kN/mm (see Figure 16). This value takes into account the axial stiffness of both the diagonal member and the connections at each end of the member. The secondary beams (parallel to Y direction) are modelled using pinned beam elements. Similar to the FEA model of the floor, the CLT slab is modelled using layered shell elements.

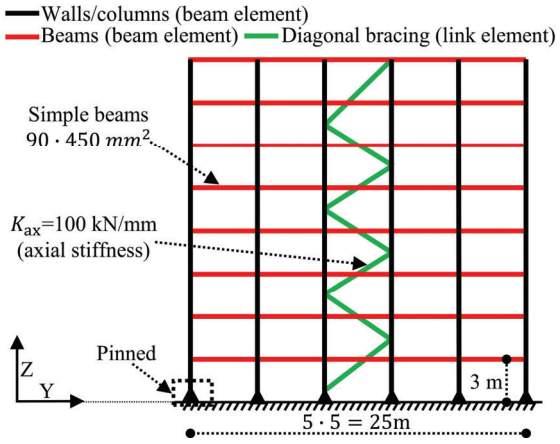

Figure 16: *2D FEA model of LLRS in Y direction*

Figure 17 shows the FEA model of the 3D structure (combining the structural systems in both X and Y). Light loads are applied to the CLT slab (Table 3). Wind loads, load combinations, parameters used for wind-induced accelerations, and cross-sections are the same as the parametric study (section 4.3, Tables 6-8).

Modal analysis of the 3D FEA model showed that the first 2 mode shapes are translational (no torsional modes). Wind-induced acceleration is calculated in X and Y directions. Figure 18 shows the accelerations against the ISO10137 [13] criterion based on 2D and 3D analyses. Wind-induced acceleration in X and Y directions meet the requirement for residential buildings.

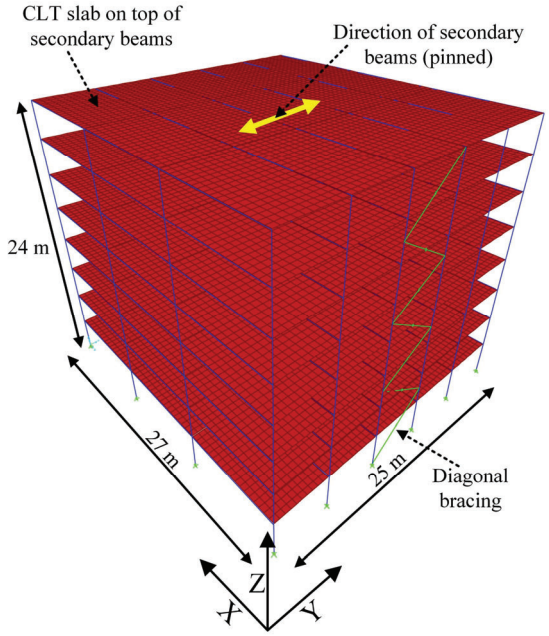

Figure 17: *3D FEA model*

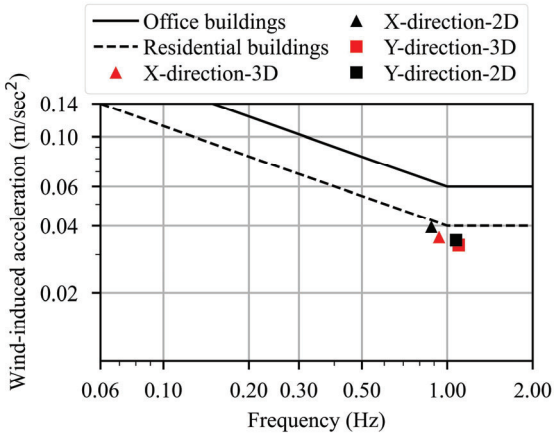

Figure 18: *Wind induced accelerations in X and Y directions of the 3D and the 2D FEA models against ISO 10137 [13] criterion*

The fundamental frequency, top floor displacement, inter-storey drift, and wind-induced accelerations of the 3D

https://doi.org/10.52202/069179-0384

model are summarized in Table 9 (both in X and Y direction). The results of the 2D counterpart model in X direction (results from section 4.3 in this paper) and Y direction are also summarized in Table 9 for comparison. The results of both 3D model and the 2D counterparts show that 2D analysis provides reasonable accuracy with the 3D model being slightly stiffer.

Table 9: *Frequency, lateral displacements, and wind-induced accelerations for the 3D FEA model and the 2D counterpart*

Direction	Property	2D	3D
X	Frequency (Hz)	0.88	0.94
	Top floor disp. (mm)	17.67	14.98
	IDR (mm)	2.61	2.18
	Acceleration (m/sec^2)	0.040	0.036
Y	Frequency (Hz)	1.07	1.10
	Top floor disp. (mm)	13.14	11.81
	IDR (mm)	2.39	2.29
	Acceleration (m/sec^2)	0.035	0.033

5 CONCLUSIONS

In this paper, a dual frame-wall structural system used as a lateral load resisting system in multi-storey timber buildings is studied. Parametric study using 2D linear elastic FEA was performed to evaluate the feasibility of the lateral load resisting system. The vibration performance of floors with respect to human-induced vibration is also discussed using linear elastic FEA. Although the main focus of the paper is on serviceability limit state, some ultimate limit state considerations are presented. To validate the results obtained from the 2D FEA model, a 3D FEA model was also prepared, and the results of both models were compared. The following conclusions are drawn (assuming wind speed of 26 m/sec and urban environment):

- Wind-induced acceleration is more critical than lateral displacements.
- Ultimate limit state is less critical than serviceability limit state. The utilization ratios of all structural elements are well below unity.
- Construction of multi-storey buildings up to 10 storeys with an out-of-plane spacing of 5 m and light flooring system is feasible if the stiffness of the beam-to-column connections is $\geq 2 \cdot 11{,}500$ kN·m/rad ($11{,}500$ for single cross-section).
- Construction of multi-storey buildings up to 12 storeys with an out-of-plane spacing of 5 m and heavy flooring system is feasible if the stiffness of the beam-to-column connections is $\geq 2 \cdot 5{,}500$ kN·m/rad ($5{,}500$ for single cross-section).
- The use of stiff connections can be optimized in such a way that stiffer connections are used in the lower storeys.
- Stiff beam-to-column connections improve the performance of the lateral load resisting system. Moreover, they also improve the performance of the floors with respect to human-induced vibration.
- The use of simplified 2D FEA modelling approach seems to give reasonable accuracy compared to 3D FEA modelling.

REFERENCES

[1] J. L. Skullestad, R. A. Bohne, and J. Lohne, "High-rise timber buildings as a climate change mitigation measure–A comparative LCA of structural system alternatives," *Energy Procedia,* vol. 96, pp. 112-123, 2016.

[2] O. A. Hegeir, T. Kvande, H. Stamatopoulos, and R. A. Bohne, "Comparative Life Cycle Analysis of Timber, Steel and Reinforced Concrete Portal Frames: A Theoretical Study on a Norwegian Industrial Building," *Buildings,* vol. 12, no. 5, p. 573, 2022. [Online]. Available: https://www.mdpi.com/2075-5309/12/5/573.

[3] A. Vilguts, H. Stamatopoulos, and K. A. Malo, "Parametric analyses and feasibility study of moment-resisting timber frames under service load," *Engineering Structures,* vol. 228, 2021, doi: 10.1016/j.engstruct.2020.111583.

[4] K. A. Malo, R. B. Abrahamsen, and M. A. Bjertnæs, "Some structural design issues of the 14-storey timber framed building "Treet" in Norway," *European Journal of Wood and Wood Products,* vol. 74, no. 3, pp. 407-424, 2016, doi: 10.1007/s00107-016-1022-5.

[5] R. Abrahamsen, "Mjøstårnet-Construction of an 81 m tall timber building," in *Internationales Holzbau-Forum IHF*, Garmisch-Partenkirchen, Germany, 2017, vol. 2017.

[6] M. Wells, "Stadthaus, London: raising the bar for timber buildings," in *Proceedings of the Institution of Civil Engineers-Civil Engineering*, 2011, vol. 164, no. 3: Thomas Telford Ltd, pp. 122-128.

[7] A. Vilguts, S. Ø. Nesheim, H. Stamatopoulos, and K. A. Malo, "A study on beam-to-column moment-resisting timber connections under service load, comparing full-scale connection testing and mock-up frame assembly," *European Journal of Wood and Wood Products,* vol. 80, no. 4, pp. 753-770, 2022, doi: 10.1007/s00107-021-01783-2.

[8] L. J. Hu and Y. Chui, "Development of a design method to control vibrations induced by normal walking action in wood-based floors," in *World Conference on Timber Engineering (WCTE2004)*, Lahti, Finland, 2004, vol. 2, pp. 217-222.

[9] P. Hamm, A. Richter, and S. Winter, "Floor vibrations–new results," in *Proceedings of 11th World Conference on Timber Engineerig (WCTE2010), Riva del Garda*, 2010.

[10] CEN, "NS-EN 14080: Timber structures-Glued laminated timber and glued solid timber-Requirements," *European Committee for Standardization: Brussels, Belgium,* 2013.

[11] CEN, "NS-EN 338: Structural timber–Strength classes," *European Committee for Standardization: Brussels, Belgium,* 2016.
[12] *CSI SAP2000 Structural analysis and design*. Computers and Structures. [Online]. Available: https://www.csiamerica.com/products/sap2000
[13] ISO, "ISO10137: Bases for design of Structures - Serviceability of Buildings and Walkways against Vibrations," *International Organization for standardization,* 2007.
[14] A. Homb and S. T. Kolstad, "Evaluation of floor vibration properties using measurements and calculations," *Engineering Structures,* vol. 175, pp. 168-176, 2018.
[15] H. Stamatopoulos, K. A. Malo, and A. Vilguts, "Moment-resisting beam-to-column timber connections with inclined threaded rods: Structural concept and analysis by use of the component method," *Construction and Building Materials,* vol. 322, 2022, doi: 10.1016/j.conbuildmat.2022.126481.
[16] CEN, "NS-EN 1991-1-1: 2002+ NA: 2019: Actions on Structures–Part 1-1: General Actions–Densities, self-weight, imposed loads for buildings," *European Committee for Standardization: Brussels, Belgium,* 2019.
[17] CEN, "NS-EN 1995-1-1:2004+A1:2008+NA:2010: Design of timber structures–Part 1-1: General–Common rules and rules for buildings," *European Committee for Standardization: Brussels, Belgium,* 2010.
[18] H. J. Blass and P. Fellmoser, "Design of solid wood panels with cross layers," in *8th world conference on timber engineering*, 2004.
[19] M. Follesa, I. Christovasilis, D. Vassallo, M. Fragiacomo, and A. Ceccotti, "Seismic design of multi-storey CLT buildings according to Eurocode 8. Ingegneria Sismica," *International Journal of Earthquake Engineering, Special Issue on Timber Structures,* vol. 30, no. 4, pp. 27-53, 2013.
[20] CEN, "NS-EN 1990:2002+A1:2005+NA:2016: Basis of structural design," *European Committee for Standardization: Brussels, Belgium,* 2016.
[21] CEN, "NS-EN 1991-1-4:2005+NA:2009: Actions on Structures–Part 1-4: General Actions–Wind Actions " *European Committee for Standardization: Brussels, Belgium,* 2009.
[22] A. Feldmann *et al.*, "Dynamic properties of tall timber structures under wind-induced vibration," in *World Conference on Timber Engineering (WCTE 2016)*, 2016.
[23] A. Gustafsson, *The CLT Handbook: CLT structures-facts and planning*, First ed. Swedish Wood, 2019.
[24] H. Stamatopoulos and K. Malo, "Wood frame solutions for free space design in urban buildings (WOODSOL)," in *Proceedings of the 7th Forum Wood Building Nordic, Växjö, Sweden*, 2018, pp. 27-28.

 https://doi.org/10.52202/069179-0384